Taylor & Francis
Taylor & Francis Group

Molecular Crystals and Liquid Crystals

ISSN: 1542-1406 (Print) 1563-5287 (Online) Journal homepage: http://www.tandfonline.com/loi/gmcl20

A BODIPY based highly selective fluorescence turn-on sensor toward VIB and IIB metal ions

Xiaochuan Li, Guangqian Ji, Jae-Myung Jung & Young-A Son

To cite this article: Xiaochuan Li, Guangqian Ji, Jae-Myung Jung & Young-A Son (2016) A BODIPY based highly selective fluorescence turn-on sensor toward VIB and IIB metal ions, Molecular Crystals and Liquid Crystals, 636:1, 159-167, DOI: 10.1080/15421406.2016.1201406

To link to this article: http://dx.doi.org/10.1080/15421406.2016.1201406

MOLECULAR CRYSTALS AND LIQUID CRYSTALS
2016, VOL. 636, 159–167
http://dx.doi.org/10.1080/15421406.2016.1201406

Taylor & Francis
Taylor & Francis Group

A BODIPY based highly selective fluorescence turn-on sensor toward VIB and IIB metal ions

Xiaochuan Li[a], Guangqian Ji[a], Jae-Myung Jung[b], and Young-A Son[b]

[a]Collaborative Innovation Center of Henan Province for Green Manufacturing of Fine Chemicals, Key Laboratory of Green Chemical Media and Reactions, Ministry of Education, School of Chemistry and Chemical Engineering, Henan Normal University, Xinxiang, Henan, P. R. China; [b]BK21, Department of Advanced Organic Materials Engineering, Chungnam National University, South Korea

ABSTRACT

A probe for recognition of IIB (Zn^{2+}, Cd^{2+}, and Hg^{2+}) and VIB (Cr^{3+}) was developed based on the framework of BODIPY. The probe was synthesized by attaching DPA to 4-position of BODIPY. It exhibited excellent sensitivity and selectivity function for the IIB and VIB metal ions with 1:1 stoichiometry in acetonitrile solution. The limit of detection of Zn^{2+}, Cd^{2+}, Hg^{2+}, and Cr^{3+} were obtained by fluorescence "turn-on" and ranged from 20.6 to 23.1 nM. Other metal cations did not interfere with the emission sensing of Zn^{2+}, Cd^{2+}, Hg^{2+}, and Cr^{3+}. The underlying mechanism of fluorescence "turn-on" is based on the intramolecular PET, which controlled the fluorescence "on" or "off."

KEYWORDS

probe; BODIPY; limit of detection; fluorescence "turn-on"; PET

Introduction

Up to now, various fluorescent organic molecules have been developed and the emission spectra run from blue to deep-red. The variation of emission color was achieved by the typically emissive molecules, such as coumarins, naphthalimide, bisindolylmalimide, perylenediimides, and rhodamine, which have been systematically engineered toward various purposes [1–11]. The application for material science and biotechnology is based on the logic input and output of optical signal. Therefore, robust fluorescent dyes are desired for chemists, physicists and biochemists. Fluorine-boron (F-B) complexes are one of the dyes and interested scientists over the past decade [12–16]. The typical example of F-B complexes is 4,4′-difluoro-4-bora-3a,4a-diaza-*s*-indacene (BODIPY), which has receive great interests. Most BODIPY dyes display a high molar extinction coefficient, narrow emission full width at half maxima (FWHM), outstanding emission quantum yields, thermal resistance, and photostability. Great efforts have been made to further improve its photochemical stability and near-infrared (NIR) emission by chemical modification of the BODIPY framework involving alkyne substitution, *N*-insertion, π-extension, etc [17–20]. Additionally, different chelating modes were also developed to expand the F-B family. In addition to the N, N complex mode of BODIPY dyes, other modes that are either ditopic (N∼C, C∼C, C∼O, O∼O) or tritopic toward borate are also well documented [21–24].

CONTACT Young-A Son yason@cnu.ac.kr Department of Advanced Organic Materials Engineering, Chungnam National University, 220 Gung-dong, Daejeon, 305-764, South Korea; Xiaochuan Li lixiaochuan@htu.cn School of Chemistry and Chemical Engineering, Henan Normal University, East Jianshe Rd. 46, Xinxiang, Henan, 453007, China.
Color versions of one or more of the figures in the article can be found online at www.tandfonline.com/gmcl.

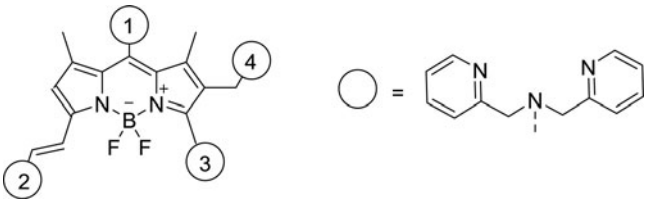

Scheme 1. Position variation of bis(pyridin-2-ylmethyl)amine in BODIPY.

Based on the framework of BODIPY, various sensor molecules were developed by attaching various chelating units [25–29]. Among them, bis(pyridin-2-ylmethyl)amine (DPA), as an well-known metal ions chelating unit, was attached to the framework of BODIPY at different position, as indicated in the following scheme [Scheme 1]. Although the chelating unit is identical to each other, the sensitivity toward to metal ions is different. According the reference report, bis(pyridin-2-ylmethyl)amine has been successfully anchored at the position of 1, 2, and 3, with which Zn^{2+}, Cd^{2+}, and Cu^{2+} were detected respectively [30–33]. Therefore, it is interesting that bis(pyridin-2-ylmethyl)amine was position-dependent in sensor design. And the switch mechanism of fluorescence signal for all of them is based on the same photoinduced electron transfer (PET). In this contribution, bis(pyridin-2-ylmethyl)amine was anchored to BODIPY at the position of 4, with which we rationalize that the more efficient PET could be occurred. And the effect of metal sensing may be different to those with the anchored units in the position of 1-, 2-, and 3-.

Experimental

General procedures and materials

The solvents used in the reaction were carefully dried according to the standard procedure and stored over 4 Å molecular sieve. All the reagent-grade chemicals were purchased from Sigma-Aldrich CO. LLC. (South Korea) and used without further purification. Melting points were determined on a Mel-Temp® IA9200 digital melting point apparatus in a glass capillary and were uncorrected. All synthesized compounds were routinely characterized by TLC and NMR. TLC was performed on aluminum-backed silica gel plates (Merck DC. Alufolien Kieselgel 60 F254).

^{1}H and ^{13}C NMR spectroscopy

^{1}H and ^{13}C nuclear magnetic resonance (NMR) spectra were recorded on a Brucker AM-400 spectrometer operating at frequencies of 400 MHz for proton 100 MHz for carbon in $CDCl_3$. Proton chemical shifts (δ) are relative to tetramethylsilane (TMS, $\delta = 0$) as internal standard and expressed in parts per million. Spin multiplicities are given as *s* (singlet), *d* (doublet), *t* (triplet), and *m* (multiplet) as well as *b* (broad). Coupling constants (*J*) are given in Hertz.

High resolution mass spectra (HRMS)

The mass spectra measured on a LC-MS (Waters UPLC-TQD) mass spectrometer. High resolution mass spectra (HRMS) were measured on a Brucker micrOTOF II Focus instrument.

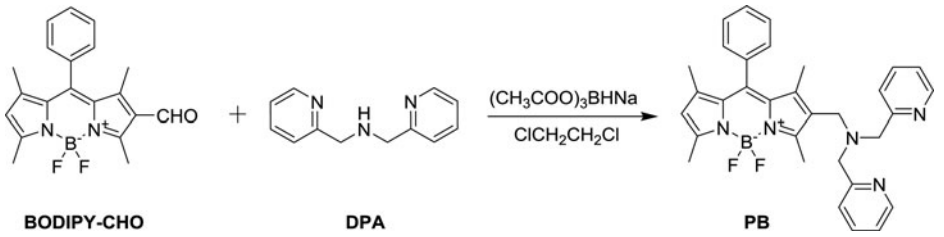

Scheme 2. Synthesis of **PB**.

UV-Vis and emission spectra

The absorption spectra were measured with a PERSEE TU-1900 and an Agilent 8453 spectrophotometer. Emission spectra were measured with Shimadzu RF-5301PC fluorescence spectrophotometer. The solvents used in photochemical measurement were spectroscopic grade and were purified by distillation. The stock solution of compounds (2×10^{-3} M) was prepared in CH_3CN, and a fixed amount of these concentrated solutions were added to each experimental solution. All the experiments were done repeatedly, and reproducible results were obtained. Prior to the spectroscopic measurements, solutions were deoxygenated by bubbling nitrogen through them.

Synthesis

Synthetic routes of the sensor, 2-*N,N*-bis(pyridin-2-ylmethyl)methanamine-BODIPY (**PB**), are outlined in Scheme 2. The aldehyde was introduced to the framework of BODIPY by standard Vilsmeier condition [34]. Subsequently, reductive amination reaction was carried out between BODIPY-CHO and DPA in the presence of sodium triacetoxyborohydride, which produced **PB**.

2-N,N-bis(pyridin-2-ylmethyl)methanamine-BODIPY (PB)

BODIPY-CHO (60 mg, 0.17 mmol) and bis(pyridin-2-ylmethyl)amine (40 mg, 0.2 mmol) were dissolved in dichloroethane (10 mL) containing sodium triacetoxyborohydride (43 mg, 0.2 mmol). The mixture was stirred in the dark overnight. After the starting materials were fully reacted, as confirmed by TLC, the mixture was neutralized by 1 N NaOH to pH ≈ 7. Next, it was extracted by dichloromethane (30 mL). The organic phase was evaporated in vacuum and the residue was loaded to the column. Chromatography separation (silica gel 200–300 mesh, eluent: dichloromethane/methanol = 100/3) produced 45 mg viscous liquid (50%).

^{1}H NMR(400 MHz, $CDCl_3$): δ (ppm): 8.43 (2 H, *s*), 7.63 (2 H, *t*, $J = 8.0$ Hz), 7.45 (3 H, *s*), 7.41 (2 H, *d*, $J = 8.0$ Hz), 7.21 (2 H, *s*), 7.13 (2 H, *s*), 5.94 (2 H, *s*), 3.73 (4 H, *s*), 3.42 (2 H, *s*), 2.51 (6 H, *s*), 1.31 (6 H, *s*). ^{13}C NMR (100 MHz, $CDCl_3$): δ (ppm): 159.0, 156.1, 155.2, 148.7, 143.1, 141.6, 141.4, 136.5, 135.1, 131.4, 130.8, 129.1, 129.0, 127.9, 123.2, 122.2, 121.2, 60.3, 48.3, 14.6, 14.3, 12.9, 12.0. HRMS (ESI): $[M+H]^+$ $C_{32}H_{32}BF_2N_5$ requires 536.2797; found $[M+H]^+$ 536.2777; and deribs $C_{20}H_{20}BF_2N_2$ requires 337.1688; found 337.1699.

Result and discussion

PB showed an intensive absorption band around 500 nm in the visible region (Fig. 1). Upon addition of various metal ions, no obvious color change was observed with 20 μM solution of **PB** in CH_3CN. Before and after the addition of metal ions, an intense absorption band

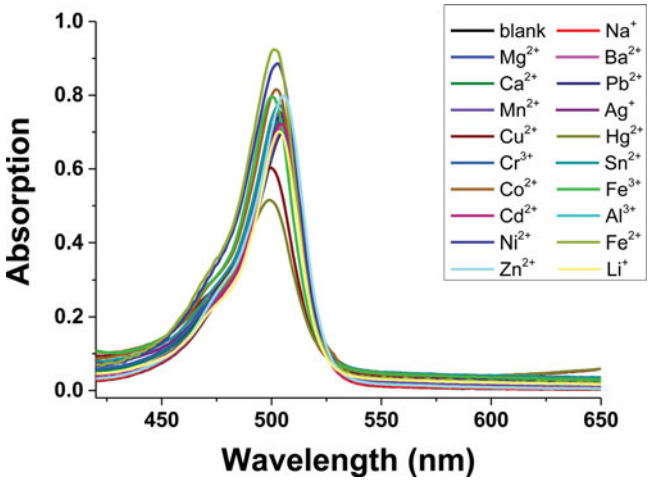

Figure 1. Absorption of **PB** (20 μM) in the presence of various metal ions (20 μM for Na^+, Mg^{2+}, Ba^{2+}, Ca^{2+}, Pb^{2+}, Mn^{2+}, Ag^+, Cu^{2+}, Hg^{2+}, Cr^{3+}, Sn^{2+}, Co^{2+}, Fe^{2+}, Cd^{2+}, Al^{3+}, Ni^{2+}, Fe^{3+}, Zn^{2+}, Li^+) in CH_3CN.

around 500 nm exhibited all the time. The blank solution of **PB** is weak emission. However, the emission intensity of **PB** in CH_3CN increased significantly with the addition of Cr^{2+}, Zn^{2+}, Cd^{2+}, or Hg^{2+}. A detailed investigation on the recognition characteristics of **PB** towards Cr^{2+}, Zn^{2+}, Cd^{2+}, and Hg^{2+} was carried out. The emission spectra of **PB** in the presence of various metal ions were shown in Fig. 2. A strong green emission (~520 nm) was induced by the addition of Cr^{2+}, Zn^{2+}, Cd^{2+}, or Hg^{2+} to **PB** in CH_3CN and only several nano meters difference was induced. In contrast, the emission intensity is similar to each other with or without other metal ions addition (Na^+, Mg^{2+}, Ba^{2+}, Ca^{2+}, Pb^{2+}, Mn^{2+}, Ag^+, Cu^{2+}, Sn^{2+}, Co^{2+}, Fe^{2+}, Al^{3+}, Ni^{2+}, Fe^{3+}, and Li^+). Generally, the DPA unit is a typical Zn^{2+} chelating unit. Together with the reference mentioned above, the chelating property of DPA is position dependent when attaching to the framework of BODIPY. It is interesting that the selectivity of **PB** with the DPA attached to the 4-position of BODIPY is not metal ion singleness. Due to

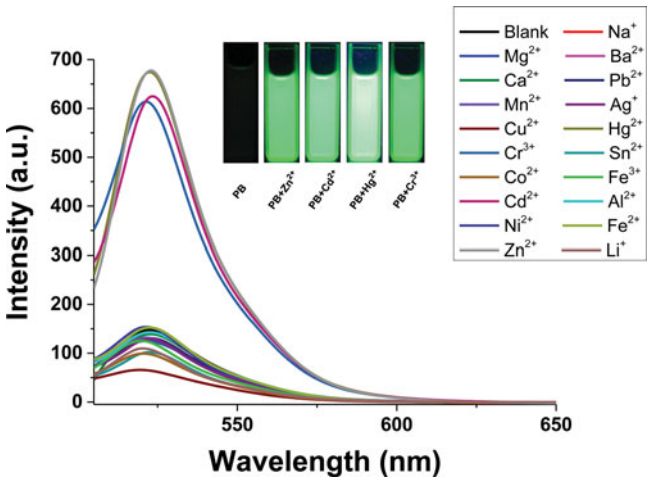

Figure 2. Emission spectra of **PB** (20 μM) in the presence of various metal ions (20 μM for Na^+, Mg^{2+}, Ba^{2+}, Ca^{2+}, Pb^{2+}, Mn^{2+}, Ag^+, Cu^{2+}, Hg^{2+}, Cr^{3+}, Sn^{2+}, Co^{2+}, Fe^{2+}, Cd^{2+}, Al^{3+}, Ni^{2+}, Fe^{3+}, Zn^{2+}, Li^+) in CH_3CN. Insert: color picture of **PB** solution with blank and addition of Zn^{2+}, Cd^{2+}, Hg^{2+}, Cr^{3+}.

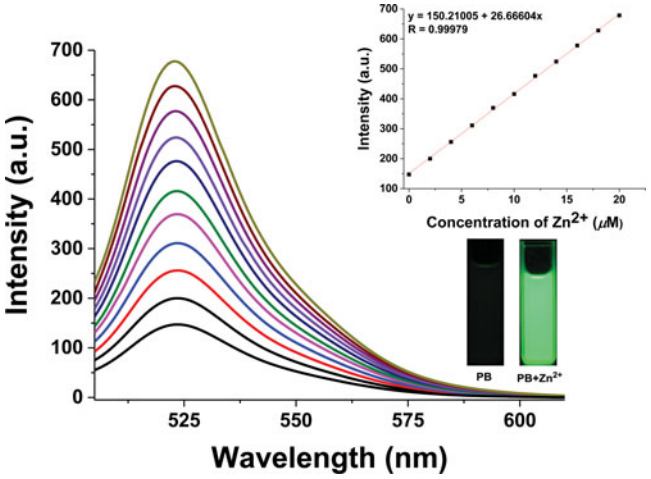

Figure 3. Changes in the emission intensity of **PB** in CH_3CN with the continuing addition of Zn^{2+} (0–1 eq). Insert: dependence of emission intensity at 523 nm with respect to the concentration of Zn^{2+} in CH_3CN.

non-existence of free metal ions of Mo and W, **PB** is selective toward to the metal ions of IIB (Zn^{2+}, Cd^{2+}, and Hg^{2+}) and VIB (Cr^{3+}). It could be ascribed to the chelation of DPA with these metal ions.

Upon addition of Zn^{2+} to the solution of **PB**, the emission maximum around 520 nm increased steadily with increasing concentration of Zn^{2+} from 0 to 20 μM (in 2 μM addition steps) with 490 nm excitation (Fig. 3). No emission wavelength shift was observed. Addition of 20 μM Zn^{2+} caused a 4.6-fold increase of the 523 nm emission signal (from 147 to 678 a.u.). A higher concentration of Zn^{2+} did not have any significant effect on the intensity of the emission signal. A satisfactory linear relationship of emission signal at 523 nm as a function of the Zn^{2+} concentration in the range of 0 to 20 μM was established with a slope of 26.666 (the correlation coefficient: 0.99979) (Fig. 3, insert). The titration experiments were repeated several times and excellent linear relationship of the emission intensity against Zn^{2+} reproduced. Based on the linear relationship between the ratio of fluorescence intensity and the Zn^{2+} concentration, the limit of detection (LOD) was then calculated with the equation: $\mathrm{LOD} = 3\sigma/m$, where σ is the standard deviation of blank measurement, m is the slope between intensity *versus* sample concentration. LOD was estimated to be 20.6 nM ($\sigma = 0.18308$), which confirmed highly sensitivity of the **PB** sensor towards Zn^{2+}.

The binding stoichiometry between **PB** and Zn^{2+} was confirmed by Job's plot (Fig. 4). Job's plot was performed by continuous variation with a total concentration of 20 μM. The emission maximum was obtained when the mole fraction of **PB** and Zn^{2+} was close to 1:1, suggesting 1:1 stoichiometry for the binding of **PB** and Zn^{2+}. To determine the association constant (*Ka*), Benesi-Hildebrand equation was used [35]. Based on the 1:1 stoichiometry supported by the Job's plot, the function was give as follows. Where F and F_0 stand for the emission intensity of **PB** in the presence and absence of Zn^{2+}, respectively; F_{max} stands for the emission intensity measured when excess amount of Zn^{2+} added; *Ka* is the association constant, $[Zn^{2+}]$ is the concentration of zinc ion added to the solution. Fig. 5 shows the Benesi-hildebrand plot and the *Ka* is calculated to be 4.95×10^4 M^{-1}.

$$\frac{1}{F - F_0} = \frac{1}{K_a\,(F_{max} - F_0)\,[Zn^{2+}]} + \frac{1}{F_{max} - F_0}$$

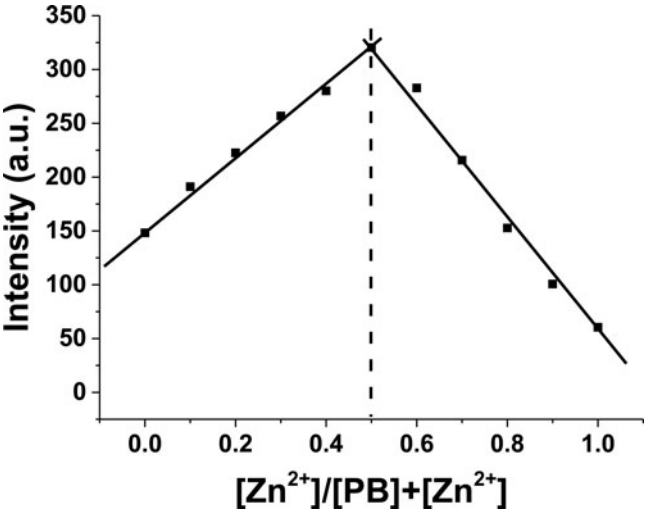

Figure 4. Job plot of **PB** and Zn^{2+} in CH_3CN. The emission was monitored at 523 nm.

The sensitivity of **PB** towards Hg^{2+}, Cd^{2+}, and Cr^{3+} were also investigated by the similar strategy to Zn^{2+}, and similar behavior was observed. All the three metal ions exhibited excellent linear relationship between the fluorescence intensity and the concentration of metal ions, and the chelation of PB to Hg^{2+} Cd^{2+}, or Cr^{3+} was in accord with 1:1 stoichiometry. The LOD of **PB** toward Hg^{2+}, Cd^{2+}, and Cr^{3+} were determined, ranging from 22.8 to 23.1 *n*M. The *Ka* ranged from 4.57×10^4 to 5.07×10^4 M^{-1}. To further explore utilization of **PB** as an ion-selective fluorescence chemosensor for IIB and VIB metal ions, a competition experiment was carried out in parallel under the same working conditions. Other metal ions mentioned in Fig. 2 were used in the competition test. Each of the metal ions was pre-incubated with **PB** before Zn^{2+}, or Cd^{2+}, or Hg^{2+}, or Cr^{3+} addition. Then the emission spectra were recorded to investigate the variation of emission intensity induced by the interference ions. As shown in Fig. 6, the emission intensity was not affected significantly in the presence of other metal ions, demonstration little interferences by other ions. Only the Cu^{2+} addition induced a slight intensity decrease, which will disturb the detection of metal contaminants in some degree.

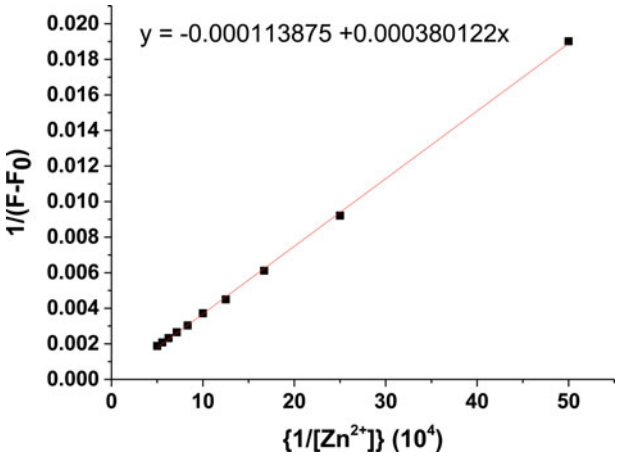

Figure 5. Benesi-hildebrand plot for **PB** with Zn^{2+} using fluorescence titration.

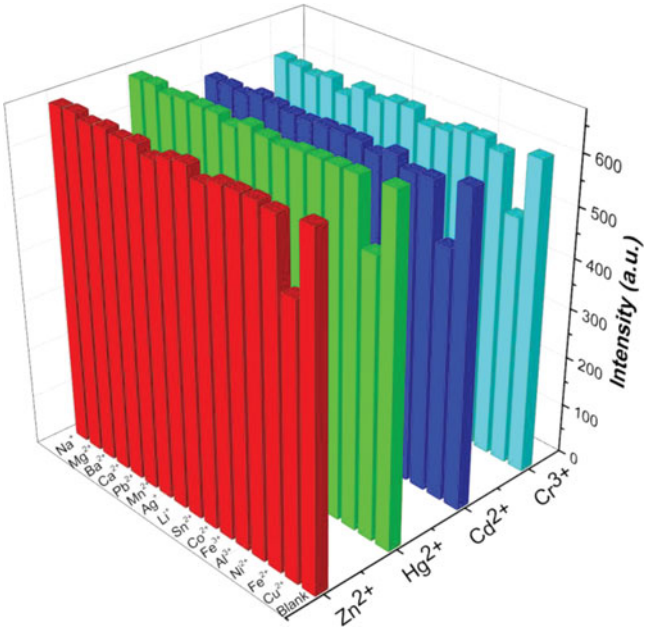

Figure 6. Emission intensity of Zn^{2+}, or Hg^{2+}, or Cd^{2+}, or Cr^{3+} in CH_3CN blended with various disturbing metal ions (Cu^{2+}, Fe^{2+}, Ni^{2+}, Al^{3+}, Fe^{3+}, Co^{2+}, Sn^{2+}, Li^{+}, Ag^{+}, Mn^{2+}, Pb^{2+}, Ca^{2+}, Ba^{2+}, Mg^{2+}, Na^{+}).

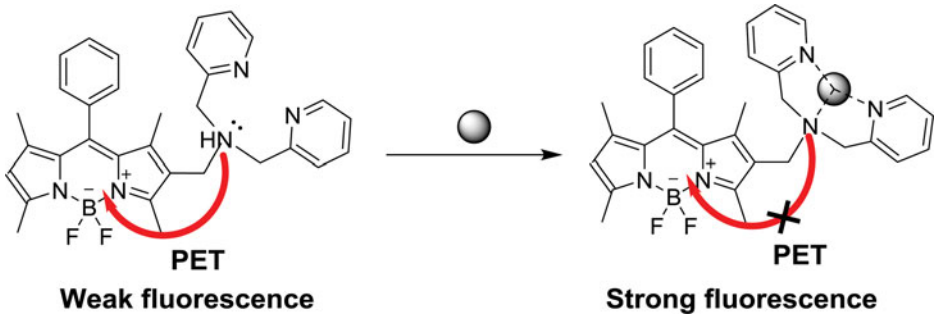

Figure 7. Metal ions triggered fluorescence "turn-on" mechanism.

Therefore, it indicates that the recognition of Zn^{2+}, Cd^{2+}, Hg^{2+}, and Cr^{3+} is selective over most of the metal ions, except for Cu^{2+}.

The fluorescence "turn-on" mechanism is based on the metal ions triggered intramolecular PET process from "off" to "on" as shown in Fig. 7. Without the chelation of metal ions, there will be efficient PET from the electron-rich *N* to the BODIPY core, which will lead to the fluorescence quenching significantly. With the metal ion harbored by DPA, the electron-donating ability will be weakened significantly. Once the PET process was blocked, the fluorescence of BODIPY was ignited again. Thus, the fluorescence "turn-on" type switch was established [36, 37].

Conclusions

In summary, a newly designed sensor with DPA attached to 4-position of the framework of BODIPY was synthesized conveniently and fully characterized. The BODIPY based sensor

PB showed highly selectivity towards IIB (Zn^{2+}, Cd^{2+}, and Hg^{2+}) and VIB (Cr^{3+}) metal ions. Upon addition the corresponding metal ion, the emission intensity increased dramatically. The recognition of Zn^{2+} by **PB** was investigated as a typical example in detail. **PB** harbors a Zn^{2+}-receptor moiety and binds in a 1:1 stoichiometry, supporting by the Job's plot. A good linear relationship was established not only for the fluoresce titration of Zn^{2+} but also for Cd^{2+}, Cr^{3+}, and Hg^{2+}. The emission LOD was ranged from 20.6 to 23.1 *n*M. Due to the effective PET from the *N* of DPA to BODIPY, **PB** is weak emission. Once the metal ion was harbored by DPA, PET was inhibited and fluorescence of **PB** was turned on. Based on the structural configuration of **PB**, more functional group could be attached to the skeleton of BODIPY in order to enhance the sensitivity, selectivity, and emission color in future molecular design. Together with the published reports, the variation of harbor units and position attached in BODIPY can be used in recognition of target metal ions. Condensation occurred at the methyl or the β-position of BODIPY could shift the emission to longer wavelength, for example red, effectively. Thus, a rough strategy on how to design various metal ions sensor can be established and developed in the future.

Acknowledgments

This work was supported by the National Natural Science Foundation of China (21272060), PCSIRT (grant no. IRT1061), and the Program for Innovative Research Team in University of Henan Province (15IRTSTHN003). This study was supported by the Basic Science Research Program through the National Research Foundation of Korea (NRF) funded by the Ministry of Science, ICT and Future Planning (Grant No. 2016901050).

References

[1] Sethna, S. M., & Shah, N. M. (1945). *Chem. Rev.*, *36*, 1.
[2] Banerjee, S., Veale, E. B., Phelan, C. M., Murphy, S. A., Tocci, G. M., Gillespie, L. J., Frimannsson, D. O., Kelly, J. M., & Gunnlaugsson, T. (2013). *Chem. Soc. Rev.*, *42*, 1601.
[3] Oelgemoller, M., & Kramer, W. H. (2010). *J. Photoch. Photobio. C*, *11*, 210.
[4] Wu, W.-C., Yeh, H.-C., Chan, L.-H., & Chen, C.-T. (2002). *Adv. Mater.*, *14*, 1072.
[5] Chen, C.-T. (2004). *Chem. Mater.*, *16*, 4389.
[6] Li, X., Xu, Y., Wang, B., & Son, Y.-A. (2012). *Tetrahedron Lett.*, *53*, 1098.
[7] Li, X., Zhao, N., Yu, L., & Son, Y.-A. (2015). *Mol. Cryst. Liq. Cryst.*, *608*, 273.
[8] Li, X., & Son, Y.-A. (2015). *J. Nanosci. Nanotechnol.*, *15*, 5370.
[9] Li, X., Zhang, J., & Son, Y.-A. (2015). *J. Nanosci. Nanotechnol.*, *15*, 5366.
[10] Ramanan, C., Kim, C. H., Marks, T. J., & Wasielewski, M. R. (2014). *J. Phys. Chem.*, *118*, 16941.
[11] Beija, M., Afonso, C. A. M., & Martinho, J. M. G. (2009). *Chem. Soc. Rev.*, *38*, 2410.
[12] Loudet, A., & Gurgess, K. (2007). *Chem. Rev.*, *107*, 4891.
[13] Ziessel, R., Ulrich, G., & Harriman, A. (2007). *New. J. Chem.*, *31*, 496.
[14] Ulrich, G., Ziessel, R., & Harriman, A. (2008). *Angew. Chem. Int. Ed.*, *47*, 1184.
[15] Li, X., Ji, G., & Son, Y. -A. (2016). *Dyes Pigm.*, *124*, 232.
[16] Li, X., & Son, Y.-A. (2014). *Dyes Pigm.*, *107*, 182.
[17] Ulrich, G., Goze, C., Guardigli, M., Roda, A., & Ziessel, R. (2005). *Angew. Chem. Int. Ed.*, *44*, 3694.
[18] Goze, C., Ulrich, G., & Ziessel, R. (2007). *J. Org. Chem.*, *72*, 313.
[19] Cheng, C., Gao, N., Yu, C., Wang, Z., Wang, J., Hao, E., Wei, Y., Mu, X., Tian, Y., Ran, C., & Jiao, L. (2015). *Org. Lett.*, *17*, 278.
[20] Jiao, L., Wu, Y., Wang, S., Hu, X., Zhang, P., Yu, C., Cong, K., Meng, Q., Hao, E., & Vicente, M. G. H. (2014). *J. Org. Chem.*, *79*, 1830.
[21] Frath, D., Massue, J., Ulrich, G., & Ziessel, R. (2014). *Angew. Chem. Int. Ed.*, *53*, 2290.
[22] Li, X., & Son, Y. -A. (2014). *Dyes Pigm.*, *107*, 1827.

[23] Chibani, S., Charaf-Eddin, A., Guennic, B. L., & Jacquemin, D. (2013). *J. Chem. Theory Comput.*, *9*, 3127.
[24] Massue, J., Frath, D., Ulrich, G., Retailleau, P., & Ziessel, R. (2012). *Org. Lett.*, *14*, 230.
[25] Isik, M., Guliyev, R., Kolemen, S., Sltay, Y., Senturk, B., Tekinay, T., & Akkaya, E. U. (2014). *Org. Lett.*, *16*, 3260.
[26] Isik, M., Ozdemir, T., Turan, L. S., Kolemen, S., & Akkaya, E. U. (2013). *Org. Lett.*, *15*, 216.
[27] Guliyev, R., Ozturk, S., Sahin, E., & Akkaya, E. U. (2012). *Org. Lett.*, *14*, 1528.
[28] Bozdemir, O. A., Guliyev, R., Buyukcakir, O., Selcuk, S., Kolemen, S., Gulseren, G., Nalbantoglu, T., Boyaci, H., & Akkaya, E. U. (2010). *J. Am. Chem. Soc.*, *132*, 8029.
[29] Ozlem, S., & Akkaya, E. U. (2009). *J. Am. Chem. Soc.*, *131*, 48.
[30] Wu, Y., Peng, X., Guo, B., Fan, J., Zhang, Z., Wang, J., Cui, A., & Gao, Y. (2005). *Org. Biomol. Chem.*, *3*, 1387.
[31] Peng, X., Du, J., Fan, J., Wang, J., Wu, Y., Zhao, J., Sun, S., & Xu, T. (2007). *J. Am. Chem. Soc.*, *129*, 1500.
[32] Atilagn, S., Ozdemir, T., & Akkaya, E. U. (2008). *Org. Lett.*, *10*, 4065.
[33] Hafuka, A., Kando, R., Ohya, K., Yamada, K., Okabe, S., & Satoh, H. (2015). *Bull. Chem. Soc. Jpn.*, *88*, 939.
[34] Jiao, L., Yu, C., Li, J., Wang, Z., Wu, M., & Hao, E. (2009). *J. Org. Chem.*, *74*, 7525.
[35] Benesi, H. A., & Hildebrand, J. H. (1949). *J. Am. Chem. Soc.*, *71*, 2703.
[36] Bozdemir, O. A., Guilyev, R., Buyukcakir, O., Selcuk, S., Kolemen, S., Gulseren, G., Nalbantoglu, T., Boyaci, H., & Akkaya, E. U. (2010). *J. Am. Chem. Soc.*, *132*, 8029.
[37] Guilyev, R., Coskun, A., & Akkaya, E. U. (2009). *J. Am. Chem. Soc.*, *131*, 9007.